J Nanopart Res (2020) 22: 47
https://doi.org/10.1007/s11051-020-4760-6

TECHNOLOGY AND APPLICATION

Combating the prevalence of water-borne bacterial pathogens using anisotropic structures of silver nanoparticles

Hala R Ali · Ahmed N. Emam · Naglaa F. Koraney · Esraa G. Hefny · Samah F. Ali

Received: 20 December 2019 / Accepted: 22 January 2020 / Published online: 10 February 2020

Abstract The current study aimed to investigate the antibacterial activity of different anisotropic structures of silver nanoparticles in the hexagon and spherical shapes against MDR-bacteria isolated from water sources in Egypt. The water samples collected from four different dairy farm-related sites were tested bacteriologically, followed by identification of the antibiotic-resistant profile for the isolates. The result revealed that *Enterococcus spp*, *Proteus spp,* and *E. coli spp* are the most common organisms in all tested water samples, and the antibiotic-resistant profile identified 11/13 waterborne isolates as MDR-bacteria. Herein, spherical and hexagonal silver nanoparticles were prepared with an average size of 26 ± 6 nm and 375 ± 80 nm, respectively, through the chemical reduction method. Further, MDR gram-positive (*Enterococcus*) and MDR gram-negative (*E. coli*) were selected for studying the antibacterial property of the synthesized AgNPs using agar well diffusion method. In another experiment, microdilution broth assay coupled with XTT assay is optimized for facilitating the testing of a broad range of AgNPs concentrations efficiently without the need for laborious preparation of the colony counting method. Our results indicated that AgNPs in spherical and hexagonal shapes are potent antibacterial against the MDR-waterborne bacteria in a dose and shape-dependent manner. The hexagonal AgNPs (h-AgNPs) express higher bactericidal activity when compared to spherical AgNPs (AgNSs) against the two tested MDR-bacteria, but the *E. coli* isolate more sensitive to both tested shapes of AgNPs than the *Enterococus* isolate. The results recommend that AgNPs can be used as efficient growth inhibitors for water-borne bacterial pathogens, making them applicable to various water filters and antimicrobial applications.

Keywords *Anisotropic structures* · *Silver nanoparticles* · *Water-borne bacteria* · Antimicrobial · Antibacterial activity · XTT assay

This article is part of the topical collection: *Nanotechnology in Arab Countries*

Guest Editor: Sherif El-Eskandarany

H. R. Ali (✉) · N. F. Koraney · S. F. Ali
Bacteriology and Immunology Department, Animal Health Research Institute (AHRI), Agriculture Research Center (ARC), Nady El-Seid St., Giza, Egypt
e-mail: alihala312@gmail.com

A. N. Emam
Refractories, Ceramics and Building Materials Department, National Research Centre (NRC), Buhouth St., 12622, Giza, Egypt

A. N. Emam
Nanomedicine and Tissue Culture Lab, Medical Research Center of Excellence, National Research Centre (NRC), Buhouth St., 12622, Giza, Egypt

A. N. Emam
Egyptian Nanotechnology Centre (EGNC), Cairo University, El-Sheikh Zayed City Campus, 6th of October City, Egypt

E. G. Hefny
Animal Health Research Institute (AHRI), Milk, and Meat Hygiene Department, Agriculture Research Center (ARC), Nady El-Seid St., Giza, Egypt

Introduction

The waterborne diseases caused by bacterial pathogens are considered a public health concern worldwide (Bush et al. 2011; Port et al. 2013). Water represents an extensive reservoir for a wide range of microbial pathogens, contamination of water sources with pathogens acts as serious health risks to all forms of life. The occurrence and spread of microbial pathogens in water sources is a warning sign of a possible outbreak of the disease not only in humans but also in animals. Water represents an essential requirement for livestock (Wakchaure and Ganguly, 2015); dairy cattle are an ideal example in their critical need to water as their total body weight is 56 to 81% water (Praveen et al. 2016). Water is highly required for dairy cows since it is the main component of milk and excretion products. A poor microbiological quality of drinking water can, therefore, adversely affect feed consumption, herd health, and productivity. Besides, public health may be compromised because livestock may serve as a source for human-hazardous pathogens, such as some strains of *E. coli*, *Yersinia enterocolitica*, and *Campylobacter jejuni* (Van et al. 2013).

The extensive and the misusage of antibiotics in human medicine, veterinary medicine, and even in agriculture resulted in the development of drug resistance bacteria (DRB) in aquatic environments. The diffusion of sewage and untreated agricultural waste in water sources is a documented way that explains the access of the DRB to water sources (Cooke 1976; Marathe et al. 2013). Thus, the exponential growth of waterborne DRB necessitates the search for an alternative to traditional antibiotics that no longer function effectively. Chlorine is the most popular disinfectant used for water purification worldwide. However, several previous studies reported that chlorination supports the activity of antibiotic-resistant bacteria (Shrivastava et al. 2004). Such studies that reported by Armstrong et al. through monitoring of a remarkable increase in DRB upon the chlorination of water (Armstrong and Calomiris, 1982; Armstrong et al. 1981). Also, Murray et al. reported that a significant increase of DRB, such as bacteria resistant to each of cefalotin and ampicillin following sewage treatment via chlorination (Murray et al. 1984). As acknowledged, it is essential to develop a new and straightforward strategy to purify water from pathogens.

In this regard, silver has been used in ancient ages to prevent spoilage of water; many stories in different ancient cultures mentioned the efficacy of silver in fighting the pathogens causing diseases (Shrivastava et al. 2004). Recently, the resurgence of silver in the form of nanoparticles with unique physiochemical properties attracts enormous research attention in various applications Ali and Selim, 2016, especially as antimicrobial agents. Several studies have been proved the potency of silver nanoparticles (AgNPs) as a microbiocidal agent (Barillo and Marx 2014; Kim et al. 2007; Rai and Yadav, 2009). The biocidal activity of AgNPs has reported against a broad range of Gram-positive and Gram-negative microorganisms, yeast, fungi, and viruses (Hamouda, 2012). The historical antimicrobial activity of AgNPs is attributed to two major pathways; first of which is the bacterial membrane that includes sulfur-containing proteins and silver nanoparticles associate with these proteins in the cell as well as phosphorous-containing compounds such as DNA. Nanoparticles prefer to attack the respiratory chain and the cellular division, eventually leading to cell death. The second pathway relates to silver ions that emerged from nanoparticles in bacterial cells which improve their antimicrobial function (Franci et al. 2015; Hamouda 2012; Sondi and Salopek-Sondi 2004).

Herein, the present work aimed to investigate the possibility of using silver nanoparticles for controlling the growth of drug-resistant bacteria recovered from water sources in dairy-related sites in Egypt. Such study has two components; *first part*, concerning isolation and characterization of bacteria from water sources including raw and tank water from sites related to dairy farms. Water sources are selected here for the current study in areas that have dairy businesses based on two concerns; first, the importance of water as an essential nutrient for all physiological processes in milking cows such as growth, reproduction, and lactation. Second, the potential risk of conversion of the milking cows to a reservoir of pathogenic bacteria upon the exposure to water contaminated with DRB. *The second part* of the work devoted for exploring the antibacterial activity for both spherical and hexagonal-like shapes of AgNPs against the DRB isolated from water samples and optimizing a new procedure using the microdilution method coupled with the XTT assay for professional screening of a wide range of concentrations without the need of laborious agar counting methods.

Materials and methods

Synthesis and characterization of anisotropic structure of silver nanoparticles

Silver nanospheres (AgNSs) were prepared via chemical reduction method, as reported by Mulfinger et al. (Mulfinger et al. 2007) with little modification. In a typical method, about 0.2 mM of polyvinylpyrrolidone (PVP, $(C_6H_9NO)_n$, Mn ~ 40,000) added to 100 ml of an aqueous solution of 47.09 mM of silver nitrate ($AgNO_3$) (Sigma Aldrich, USA) under vigorous stirring and dark conditions. After 15 min, about 10 ml of a 10 mM ice-cooled aqueous solution of sodium borohydride ($NaBH_4$, 85%, WinLab Ltd) was injected dropwise into the reaction vessels. Whereas, hexagonal-like shape silver nanoparticles (*h*-AgNPs) are prepared with the same experimental conditions for the spherical nanoparticles with a change in the molar ratio of $AgNO_3$/PVP-40 K = 188.36. The resultant colloidal solution was stirred for 1 h and aged for 24 h before use.

The synthesized particles were characterized using high-resolution transmission electron microscopy (HR-TEM) JEM 2100 LB_6 under an operating voltage of 200 kV to investigate the micrograph of as-prepared *S*-AgNPs and *h*-AgNPs. The photophysical properties such as UV-Vis absorption and emission have been investigated using TG80 (PG instruments) double beam UV-Vis spectrophotometer. The absorption spectra were recorded within the appropriate scan range from 250 to 900 nm. Furthermore, colloidal properties, including particle size distribution and zeta potential were measured by dynamic light scattering (DLS) using Malvern Zetasizer Nano-ZS (Malvern Instruments Ltd., Worcestershire, UK). Finally, the surface properties such as, the visible surface-enhanced Raman (SERS) spectra were recorded in the range from 250 to 3500 cm^{-1} using a LabRAM HR 800 (Horiba/Jobin Yvon, Longjumeau, France) laser Raman analyzer, which equipped with a frequency-doubled Nd:YAG 532 nm laser. Also, the FT-IR spectra were recorded in the range from 500 to 4000 cm^{-1} using Thermo Nicolet 6700 Fourier transform infrared spectrometer (FT-IR).

Sampling

Raw water samples, as well as tank water samples from the dairy farm, which collected from four different sources in Egypt. Raw water samples from agricultural and farm water sources were collected aseptically in sterile 1000 ml glass bottles by directly dipping the bottles into the surface of the water. Tank water samples were collected directly into the sterile bottles from the tap after allowing the tap to run 60 s. The samples were labeled and transported in an icebox to the laboratory for analysis. Then, the samples used for selective isolation of *fecal coliforms, S .aureus, Pseudomonas*, and *Enterococcus faecalis* based on standard bacteriological procedures (Bibo et al. 2012).

Bacterial isolation and characterization

Isolation using filter paper filtration

The collected samples with a volume of 100 ml have filtered via sterile filter paper. The used sterile filter papers are then aseptically introduced into test tubes containing 5 ml Buffered Peptone Water (Difco), and then incubated overnight at 37 °C. Then, from each tube, 1 ml of broth was transferred into each of the different plates with appropriate selective media. The selective media used are as follows: MacConkey agar used as a selective medium for *fecal coliforms*, Baird-Parker medium for *S. aureus*, and Bile Ausculine agar for *Enterococcus Faecali*. All the used media have prepared according to instructions recommended by the supplier. The samples have analyzed in triplicate. All sampling plates were incubated at 37 °C for 24 h. The obtained colonies such as pink colonies from MacConkey agar (*presumptive coliform*), black colonies from Baird-Parker (*presumptive S. aureus*), and green colonies (*presumptive Pseudomonas*) are morphologically characterized.

Characterization of bacterial species

The isolated pure bacterial colonies identified and characterized by using standard bacteriological methods. First, all isolates were subjected to biochemical analysis methods, including carbohydrate fermentation test, oxidase test, coagulase, catalase, indole, methyl red, Voges Proskauer, citrate utilization, and urease. Then, their ability to produce hemolysis on blood agar was performed. Blood agar (Sigma, Egypt) supplemented with 5% sheep blood was determined after the incubation of the plates at 37 °C for 24 h. Hemolysis is identified by streaking the isolates on a blood agar plate. After incubation, the medium was examined for signs of alpha or

beta-hemolysis. Discoloration of the medium or darkening after growth, the organism was considered alpha-hemolytic, while appearance of a clear hollow under growth constitutes beta-hemolysis. Gamma hemolysis was demonstrated with a lack of any change in the medium color after growth (Köhler 1975; Mulamattathil et al. 2014).

Preparation of bacterial suspensions

The bacterial colonies from each sample were transferred into a tube containing sterile saline for preparing a bacterial suspension, and then each bacterial suspension was adjusted to 0.5 McFarland standards.

Antibiotic sensitivity testing

The antibiotics sensitivity study was performed using the Kirby-Bauer disk diffusion method (Bauer et al. 1966). All the isolates were tested against: cefuroxime (CXM) 30 mcg, tobramycin (TOB) 10 mcg, rifampin (RA) 5 mcg, chloramphenicol (C) 30 mcg, ofloxacin (OFX) 5 mcg, trimethoprim/sulfamethoxazole (SXT) 25 mcg, amikacin (AK) 30 mcg, and vancomycin (VA) 30 mcg. These antibiotics were selected for this study because they are extensively used in human and veterinary medicine. The 100 L from each bacterial suspension that previously prepared were spread plated on Mueller Hinton agar plates. Antibiotic discs were applied to the plates using sterile needles, and the plates were incubated at 37 °C for 24 h. After incubation, the interpretation of inhibition zones around the disks was according to CLSI (Clinical, Institute LS, 2009).

Antibacterial activity of AgNPs against *Gram-positive* and *Gram-negative* bacterial isolates (*Enterococcus spp*. and *E. coli,* respectively)

Agar well diffusion method

Similarly to the method used in the disk diffusion method, all agar plates are inoculated by spreading a fixed volume of the bacterial inoculum over the entire agar surface. Then, a hole with a diameter of 6 to 8 mm is created aseptically with a sterile, a tip or cork borer, and the tested AgNPs concentration diluted in a 100 μL volume of Muller Hinton broth inserted into the well. For the untreated control, only 100 μL of Muller Hinton broth added in the hole. After that, all agar plates are incubated for 24 h at 37 °C, and they are examined for the zones of inhibition (Patel et al. 2011).

Microdilution broth assay coupled with XTT assay

Microdilution broth assay To detect the antibacterial activity of AgNPs and the minimum inhibitory concentration (MIC), microdilution broth method was performed according to CLSI in 96 well plates and incubated at 100 μl of Muller Hinton broth was added in each well, followed by adding 60 μl of broth plus 40 μl of NPs in each well of column number 3. Serial dilutions were performed from column 3 to column 11 to obtain the final NPs concentrations ranging from 200 μg/mL to 0.78 μg/mL. A 100 μL of bacterial suspension was added to each well except all wells of column numbers 1 and 2, making the final volume of 200 μL. Wells of column 1, containing inoculum and formaldehyde act as negative growth control, but column number 2 containing the only medium, act as the control medium. While wells of column (12), act as a positive growth control containing nanoparticle – free medium and inoculum. All plates have incubated at 37 °C for 24 h.

XTT assay: The XTT cell viability assay kit according to the manufacturer's protocol, following incubation of the treated bacterial isolates in the 96 well plates that previously subjected to microdilution broth method, 125 μL of XTT solution was added to all wells of each plate. Then, all the 96 well plates were incubated at 37 °C for 6 h. Then, the optical density was measured at 450 and 690 nm using A Biotek Synergabsoy H4 multi-mode plate reader. The error bar is expressed as ± the percent relative standard deviation (% RSD).

Results and discussion

Anisotropic structures of silver nanoparticles: synthesis and characterization

Silver nanoparticles with spherical-like shape were prepared via chemical reduction of silver salts (i.e., $Ag^{+}NO_3^{-}$) using $NaBH_4$, which acts as reducing and in the presence of PVP-40 K as capping agent that prohibiting aggregation and further grain growth as a result of steric effect arising from the long polyvinyl chain of PVP (Mulfinger et al. 2007). The appearance of the brownish-yellow color was evident for the formation of silver nanospheres. In such a case, adsorption of

borohydride (BH_4^-) plays a crucial role in stabilizing growing AgNPs, providing a particle surface charge (Singh et al. 2015), as shown in Equ. 1

$$AgNO_3 + NaBH_4 \rightarrow Ag + {}^{1}/_{2}B_2H_6 + NaNO_3 \quad (1)$$

As shown in (Fig. 1, Black-line), spherical AgNPs exhibit a single narrow of the surface plasmon band (SPR) at 415.7 nm which indicates that prepared particles are the almost spherical-like shape as confirmed by TEM micrographs (see Fig. 2a and b). The TEM image shows the average size of spherical Ag NPs were around 26 ± 6 nm. Based on our knowledge, the number of SPR peaks increases as the symmetry of particles decreases (Das and Das, 2010; Singh et al. 2015). Therefore, on further increasing the concentration of PVP-40 K, where the ($AgNO_3$/PVP-40 K) molar ratio decreased from 235.4 to 188.36, two further optical features corresponding to transverse, and quadrupole bands that are started appearing at 347.5 and 377.4 nm, respectively. Moreover, the longitudinal SPR band has a redshift in position at 438.9 nm (Fig. 1, Red-line and Inset). Also, their broadening was attributed to the increase in particle size and change in the particle shape that confirmed by TEM micrographs, as shown in Figs. 2c and d. Furthermore, the FWHM increases as particle size distribution increases. It is clear that the prepared particles are almost hexagonal-like shapes, and the average size in diameter was around 255 ± 50 nm and 375 ± 80 nm of edge length. Our observations were in agreement with Harada (2007), which suggested that any change in the concentration of capping agents (i.e., PVP-40 K) followed by change and variation in both size and shape.

Furthermore, dynamic light scattering (DLS) and electrophoretic mobility for as-prepared samples (i.e., *S*-AgNPs and *h*-AgNPs) in a vehicle solution are represented in Table 1. *S*-AgNPs showed the smallest size, where the hydrodynamic diameter (H_D) was about 54.54 ± 10.98 nm with a polydispersity index (PDI) 0.28, and the lowest zeta potential that was about 0.27 ± 4.42 mV. Whereas, *h*-AgNPs showed the dominant size (see Fig. 3 and Table 1). The average hydrodynamic diameter was about 275.6 ± 93.05 nm. Moreover, the corresponding zeta-potential was about −0.94 ± 6.55 mV, as shown in Fig. 3 and Table 1.

Finally, the surface properties of as-prepared PVP-capped AgNPs spherical and hexagonal shapes have been investigated via surface-enhanced Raman spectroscopy (SERS) and diffused reflectance as function

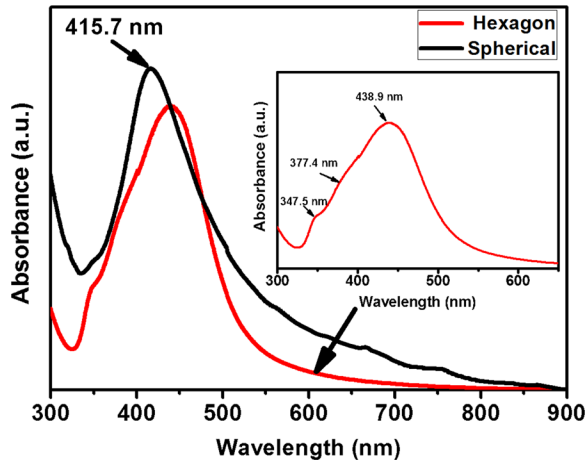

Fig. 1 The absorption spectra of as-prepared silver nanostructures in both spherical (Black-line) and hexagonal (Red-line)-like shapes. The inset showed the distinct features of silver NPs with hexagons' shape

in wavenumber by Fourier-transform infrared (FT-IR) as shown in Figs. 4 and 5, respectively. As shown in Fig. 4, the SERS spectra of spherical AgNPs shows multiple bands within the range from 500 to 2500 cm^{-1}. In such a case, three bands at 1340.79, 1459.35, and 1573.52 cm^{-1} that characteristic to spherical AgNPs (see Fig. 4a). Whereas, the hexagonal AgNPs also exhibited three-characteristic bands with a slight Raman shift at 1353.93, 1416.19, and 1566.69 cm^{-1}; besides a remarkable enhancement in SERS signal compared to spherical shapes (see Fig. 4b), which is due to localized field enhancement at the tips of hexagonal shape. In contrast, both spherical and hexagonal shapes of AgNPs shows the same diffused reflectance; FT-IR showed the same strong stretching bands at wavenumbers of 2526.3 and 3031 cm^{-1} due to the presence of –OH (carboxylic acid) and –NH (amine salt), respectively, exist in PVP molecules (see Fig. 5).

Isolation and characterization of water-borne bacteria

Thirteen bacterial isolates were recovered from raw, and Tank water sources at five different sites belong to dairy farms in Egypt. The isolates were selected for biochemical analysis and hemolytic reaction followed by the drug sensitivity study to detect their antibiotics resistance profiles. As shown in Table 2, our result of biochemical analysis and hemolytic reaction identified the isolates as (4/13) *E. coli*, 4/13 *Enterococcus spp*,

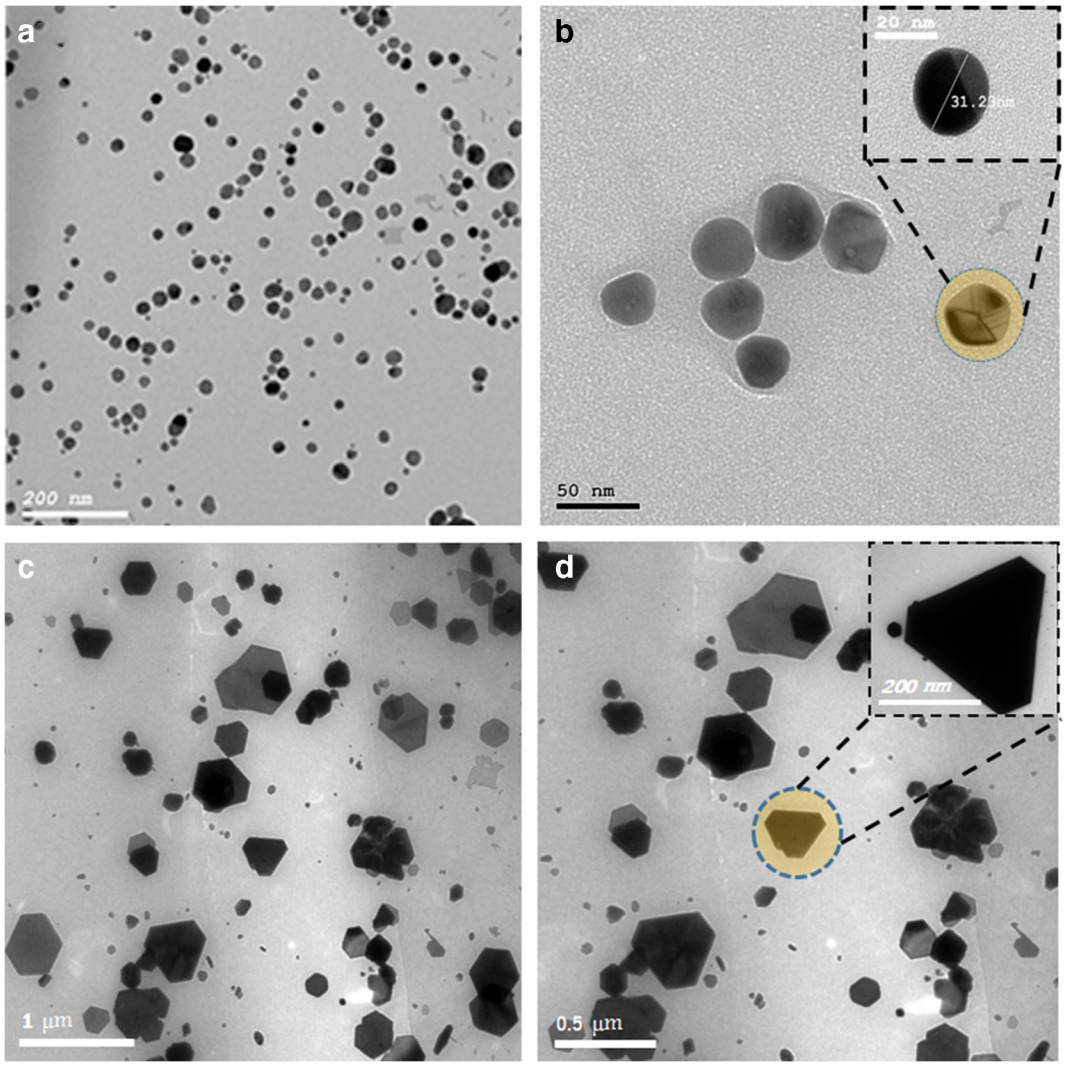

Fig. 2 TEM micrographs for anisotropic structures of silver nanoparticles **a** and **b** spherical and **c** and **d** hexagonal-like shapes at different magnification power

2/13 *S. aureus*, 2/13 *Pseudomonas spp,* and 1/13 *Proteus spp*. Also, we observed that *E. coli* and *Enterococcus spp* are the most common bacteria in both raw and tank water, whereas *S. aureus* bacteria are detected only in the raw water samples.

Table 1 The colloidal properties of tested vehicles

Sample	Dynamic Light Scattering Data		Zeta-potential, mV
	H_D, *nm*	PDI	
S-AgNPs	54.54 ± 10.98	0.28	0.275 ± 4.42
h-AgNPs	275.6 ± 93.05	0.210	−0.94 ± 6.55

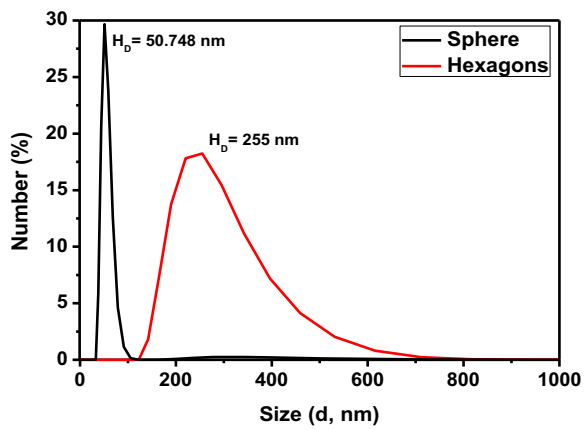

Fig. 3 Dynamic Light Scattering (DLS) curves of **a** Spherical **b** and hexagonal-like shapes of silver nanoparticles (AgNPs)

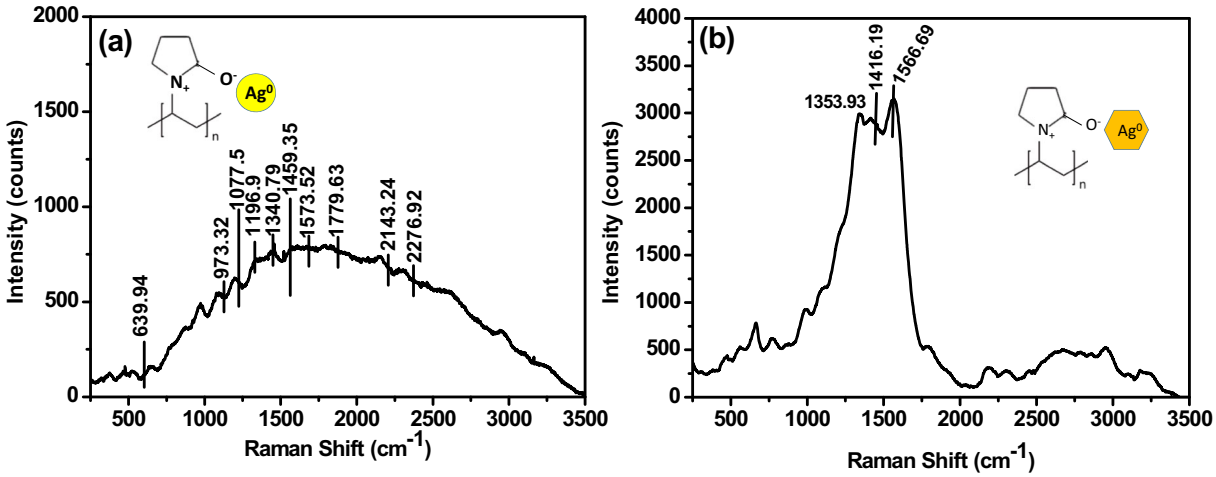

Fig. 4 Surface-enhanced Raman spectra (SERS) for as-prepared AgNPs with. **a** Spherical. **b** and hexagonal-like shapes

Recovering *E. coli* from drinking water (tank water) is a strong indication of sewage or human and animal waste contamination (Hamouda 2012). The presence of fecal coliforms, particularly *E. coli* in drinking water, is the primary method for water assessment. *Enterococci* are also used as indicators of fecal contamination of drinking water throughout the world (Hoadley and Dutka 1977); they are not permitted in a volume 100 mL sample of tested drinking water that flows from a tap according to the European Union (EU) (Köhler 1975). Although *S. aureus* is one of the most common foodborne pathogens, and the causative agent of a variety of illness (Boehm and Sassoubre 2014), their incidence in water samples is unexpected. Their presence in our water sample might indicate a risk of intoxications.

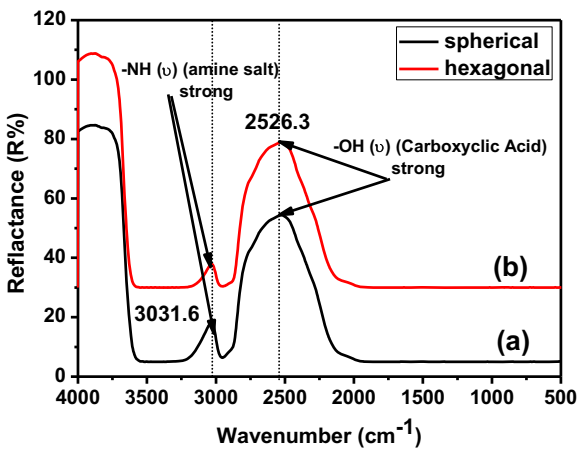

Fig. 5 Diffused reflectance as a function in wavenumber for as-prepared AgNPs with. **a** Spherical. **b** and hexagonal-like shapes

To detect multidrug-resistant (MDR), extensively drug-resistant (XDR) among water-borne bacterial isolates based on the common term of MDR in many previous studies, that refers to MDR by acquired in vitro resistance to ≥3 classes of antibiotic (Ljujic and Sundac), the antimicrobial susceptibility analysis was performed using the Clinical Laboratory Standard Institute (CLSI) disc method. The *Gram-negative* isolates were tested against 15 antimicrobials belonging to 10 antimicrobial categories, while the *Gram-positive* isolates were tested against 16 antimicrobials belonging to 11 antimicrobial categories. The antibiotic resistance results listed in Table 3, based on the resistance phenotype definition, we isolated 11 MDR bacteria: 3/4 bacteria were identified as *E. coli*, 1/1 bacteria are identified as Proteus, 2/2 bacteria were identified as Pseudomonas, 3/4 bacteria are Enterococcus, and 2/2 bacteria are *S. aureus* (Magiorakos et al. 2012).

The assessment of the antibiotic-resistant profile of all the waterborne bacterial isolates revealed that most of the isolates experienced resistant to a wide range of antibiotics. As shown in Fig. 6, about 84.6% of isolates were resistant to oxytetracycline and ampicillin-sulbactam. In addition, 76.9% of isolates were resistant to cefuroxime, and 69.3% of isolates were resistant to amoxicillin-clavulanate and colistin. Moreover, about 46.1% of isolates were resistant to cefepime, cefotaxime, tobramycin, and aztreonam. Furthermore, 38.6% of isolates were resistant to rifampicin; 30.7% of isolates were resistant to ciprofloxacin and doxycycline. Finally, 15.3% of the isolates were resistant to amikacin, and 7.6% of the isolates were resistant to vancomycin and ofloxacin.

Table 2 Characterization of water-borne bacterial isolates using biochemical analysis and hemolytic interaction on blood agar (Stiles and Ng 1981)

Biochemical tests		The carbohydrate fermentation test					Catalase	coagulase	Indole	Methyl red	Voges Proskauer	Citrate Utilization	Oxidase	Urease	Blood agar
		Dextrose	Maltose	Lactose	Sucrose	Manniol									
Bacterial Isolates	*E. coli*	+ AG	+ AG	+ AG	+ AG	+ AG	+	–	+	–	–	–	–	–	either α- or β--haemolysis
	S. aureus	+A	+A	+A	+A	+A	+	+	–	–	–	+	–	+	β-haemolysis
	Pseudomonas spp.	NT	–	–	–	+	+	–	–	–	–	+	+	–	β-haemolysis
	Enterococci spp	NT	+	+	+	+	–	–	–	–	+	–	–	–	β-haemolysis
	Proteus spp	–	+	–	+	–	+	–	–	+	–	–	–	+	β-haemolysis

AG, Production of acid and gas; +ve, positive reaction; −ve, negative reaction; and NT, not tested

Table 3 The antimicrobial resistance profile of the waterborne bacterial isolates performed according to the Clinical Laboratory Standard Institute (CLSI) disc method 2

Antimicrobial category	Antimicrobial Agent / Disk content	Bacterial Isolates									
		Gram-negative isolates						*Gram-positive* isolates			
		E. coli		*Proteus spp*		*Pseudomonas spp*		*Enterococcus spp*		*S. aureus*	
		T	R %	T	R%	T	R %	T	R %	T	R%
Non-extended spectrum cephalosporins; first and 2nd generation	Cefuroxime 30 μg	4	4 (100)	1	1 (100)	2	2 (100)	4	1 (25)	2	2 (100)
Extended-spectrum cephalosporins; 3rd and 4th generation	Cefotaxime 30 μg	4	1 (25)	1	0	2	1 (50)	4	1 (25)	2	2 (100)
	Cefepime 30 μg	4	1 (25)	1	1 (100)	2	1 (50)	4	1 (25)	2	2 (100)
Fluoroquinolones	Ofloxacin 5 μg	4	0	1	0	2	0	4	1 (25)	2	0
	Ciprofloxacin 5 μg	4	2 (50)	1	0	2	1 (50)	4	2 (50)	2	1 (50)
Tetracycline	Doxycycline 30 μg	4	0	1	0	2	2 (100)	4	1 (25)	2	1 (50)
	Oxytetracycline 30 μg	4	3 (75)	1	1 (100)	2	2 (100)	4	4 (100)	2	2 (100)
Folate pathway inhibitors	Trimethoprim/sulfamethoxazole 1.25/23.75 μg	4	0	1	0	2	0	4	2 (50)	2	2 (100)
Aminoglycosides	Tobramycin10 μg	4	1 (25)	1	1 (100)	2	2 (100)	4	3 (75)	2	0
	Amikacin30 μg	4	1 (25)	1	0	2	0	4	1 (25)	2	0
	Kanamycin30 μg	4	4 (100)	1	1 (100)	2	2 (100)	NT	NT	NT	NT
Beta-lactam/beta-lactamase inhibitor	Amoxicillin-clavulanate10/20 μg	4	2 (50)	1	1 (100)	2	2 (100)	4	4 (100)	2	0
	Ampicillin-sulbactam 20 μg	4	3 (75)	1	1 (100)	2	2 (100)	4	3 (75)	2	2 (100)
Phenicols	Chloramphenicol l30 μg	4	1 (25)	1	0	2	0	4	0	2	2 (100)
Glycopeptides	Vancomycin	NT	NT	NT	NT	NT	NT	4	0	2	1 (50)
Monobactams	Aztreonam 30 μg	4	3 (75)	1	1 (100)	2	2 (100)	NT	NT	NT	NT
Ansamycins	Rifampin5 μg	NT	NT	NT	NT	NT	NT	4	3 (75)	2	2 (100)
Lipopeptides	Colistin 10 μg	4	2 (50)	1	1 (100)	2	2 (100)	4	3 (75)	4	1(25)

T, tested; NT, not tested; and R, resistant

S, sensitive; R, resistant; and NT, not tested

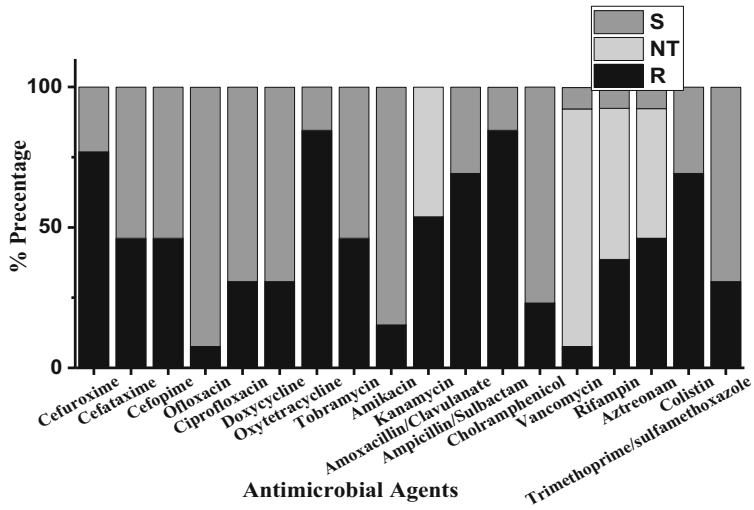

Fig. 6 Antibiotic resistance profiles (%) among the bacterial isolates from water samples collected in 2017 from four different sites used for watering dairy cows in Fayoum City, Egypt

S: sensitive, R: resistant and NT: Not Tested

The presence of MDR-bacteria in the aquatic environment is a sign of alarm for the potential outbreak of bacterial infections that indeed lead to a sharp increase in mortality, morbidity, and the cost of prolonged treatments. Although chlorination is the standard method used to purify water, some previous studies have shown a significant increase in the proportion of MDR- bacteria following chlorination (Barillo and Marx 2014; Kim et al. 2007; Rai and Yadav, 2009; Shrivastava et al. 2004; Sondi and Salopek-Sondi 2004). It is, therefore, highly relevant to alternative agents for prevention the prevalence of these pathogenic bacteria in the water. Hence in the present work, our next concern is investigation the antibacterial activity of two different geometry of silver nanoparticles against MDR- waterborne isolates, a model of *gram-positive (Enterococcus*), and a model of *gram-negative (E. coli)*.

The antibacterial activity of silver nanoparticles

The antibacterial property of silver is well-known for many years. It shows a promising antimicrobial property in comparison to other nanoparticles. Therefore, multiple studies investigated their efficacy against microbes in order to face the continuous growth in antimicrobial resistance. The two different methods assessed the antibacterial activity of silver nanoparticles, the agar well diffusion method, and the microdilution method using XTT. The two MDR-isolates (*E. coli* and *Enterococcus spp*) were selected for exploring the antibacterial power of the synthesized AgNPs. These isolates were selected based on their public health hazard and their involvement in pathogenic illness in humans and animals as well as their antibiotic-resistant profiles (Fig. 7).

The result of the well diffusion method revealed that both shapes of AgNPs inhibit the bacterial growth of the tested isolates in a dose-dependent manner. The tested concentrations were 10, 20, 50, 100, and 200 μg/ml, and the zone of inhibition produced by both shapes of AgNPs against *E. coli* isolates was 2.4, 2.6, 2.7, 2.9, and 3 cm, respectively. While the zone of inhibition produced by the same concentrations was 2, 2.2, 2.4, 2.5, and 2.7 cm for *Enterococcus* isolate, respectively (Fig. 8). The *E. coli* found to be more susceptible to AgNPs than the enterococcus isolate; however, the shape of AgNPs showing no difference in the efficacy. This result might be due to the activity of particles in this experiment, depending on the direct contact of a particle with bacteria

As clarified in Fig. 9, different steps of our optimized method were stated, starting from developing the double fold dilution of the tested NPs till adding the XTT solution and monitoring the reduction of XTT to orange product (formazan dye) (Riss et al. 2016). First, the tested AgNPs were serially diluted in 96-well plates (See Fig. 9A); then we measured the absorbance at 450 nm and 960 nm *reading* (**I**). Further, the tested bacterial suspension was added to all the wells except columns 1 and 2, which are considered negative growth control and medium control, respectively. After that, the 96-well plate incubated for 24 h (see Fig. 9B) followed by adding the XTT solution. Then after 6 h of XTT

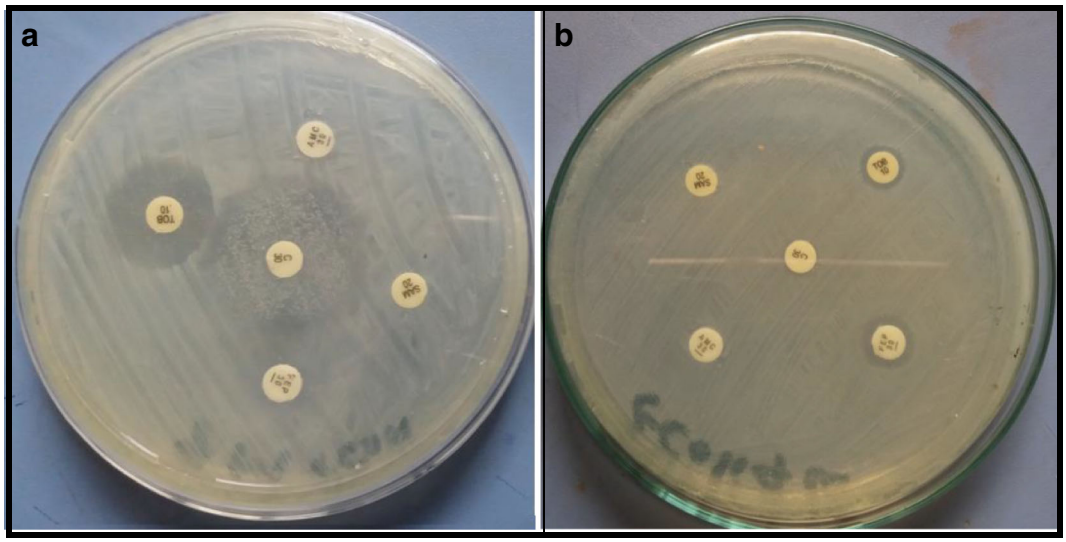

Fig. 7 Disk diffusion method. Muller Hinton agar plates inoculated with bacterial suspension, then the antibiotics disk (chloramphenicol, Amoxicillin/clavulanic acid, Ampicillin/Salbactum, Cefepime, and Tobramycin) are placed followed with incubation of the plates at 37 °C for 24 h. **a** *Enterococcus* isolates. **b** *E.coli* isolates

treatment, the absorbance was measured again at 450 and 960 nm *reading* (**II**), then *reading* (**I**) subtracted from *reading* (**II**) to remove the background of the particles. The visual inspection of the plate shown after that 24 h incubation of the inoculum with different dilutions of NPs, macroscopic turbidity was only observed in the lowest NPs concentrations (3.12, 1.56, and 0.78 μg/ml) and untreated control that represented in columns 9–12, respectively (see Fig. 9B). While after 3 h and 6 h of adding XTT mixture, the intensity of orange-red color increased in columns 9–12 as the concentration of particles decreases (see Fig. 9C and 9D), which is indicative to decreasing viability of the bacteria in a dose-dependent manner. This visual observation is further confirmed by measuring the absorbance of 96-well plates, where the data indicated that AgNPs exhibit a strong antibacterial effect against the tested bacteria.

The antibacterial effect of the AgNPs is not only dose-dependent but also is shape-dependent, where the h-AgNPs have shown a more significant antibacterial effect than the spherical shape. The XTT result demonstrated that the MIC of h-AgNPs to *E. coli* and *Enterococcus* isolates are 6.25 and 25 μg/ml, respectively, while the MIC of AgNSs to *E. coli* and *Enterococcus*

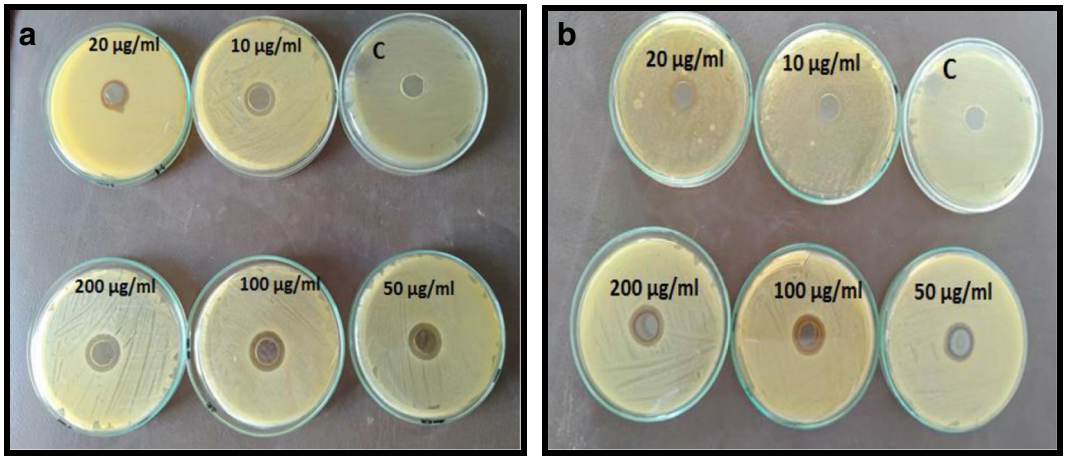

Fig. 8 The agar well diffusion method for testing the antibacterial activity of h-AgNPs. An overnight culture of *Enterococcus* isolates. **a** or *E.coli* isolates. **b** are spread on the agar plates, a well created in the agar, and different concentrations of NPs diluted in Muller Hinton broth or saline (control) were placed in the wells

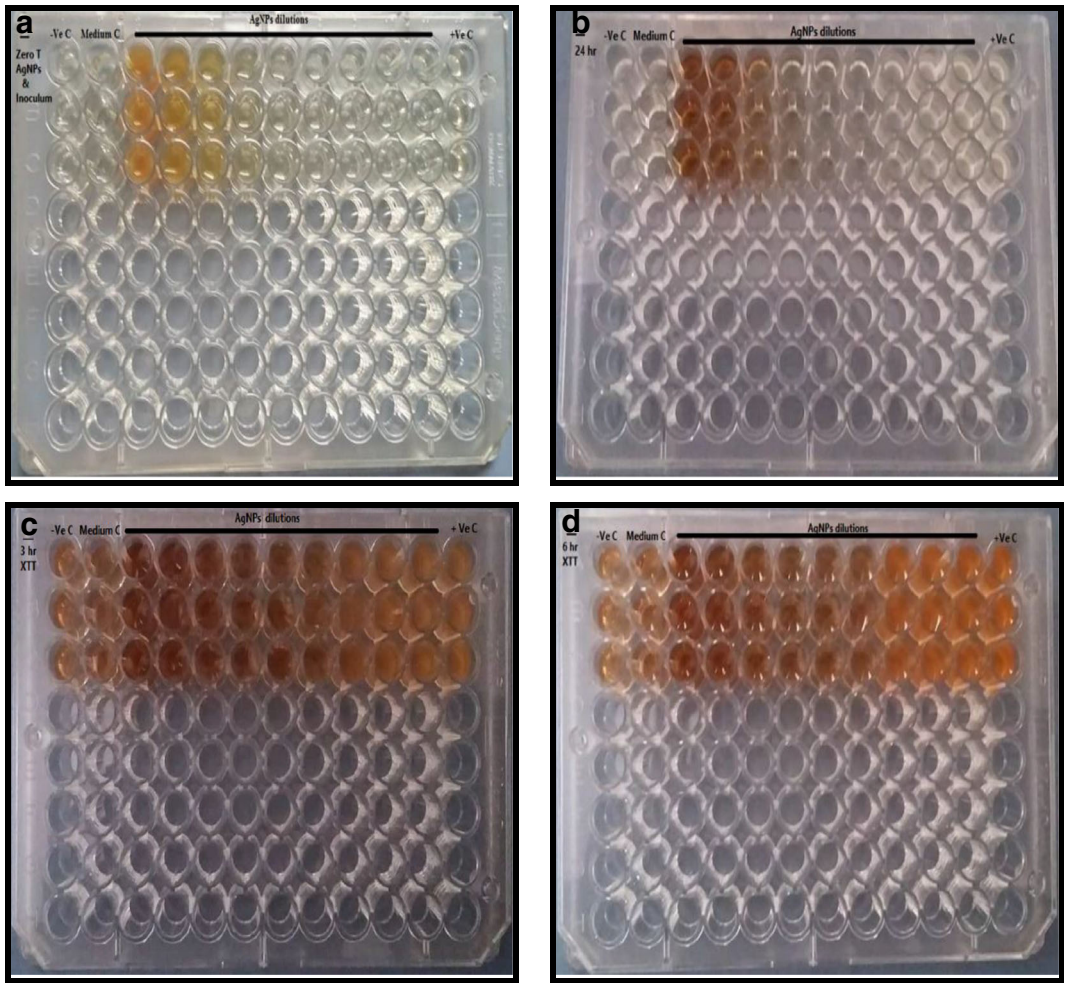

Fig. 9 Ninety-six well Microtiter plates of the colorimetric-XTT assay. The different steps of testing the antibacterial activity of AgNPs using the broth microdilution method where AgNPs were serially diluted from column 3 to 11 while column 1 is -ve growth control (formaldehyde + inoculum), column 2 is medium C (inoculum -free), and column 12 is NPs-free (+ ve growth control). **a** The image of the plate showing the zero time of adding the inoculum to the different dilutions of NPs. **b** showing the image of the plate captured after 24 h incubation. **c** and **d** are the images of the plate after 3 h and 6 h incubation with the XTT mixture, respectively

isolates are 12.5 and 50 μg/ml, respectively, as shown in Fig. 10.

The nanoparticle's shape seems to play an important role in exploring their antimicrobial nature (Ali et al. 2016). Silver nanoparticles (AgNPs) with different anisotropic structures have shown varying degrees of antimicrobial activities, which are attributed to different degrees of interactions between the bacterial cell and nanoparticles, thus, damaging the bacterial membrane and DNA. In this regard, several studies have been devoted to investigating antibacterial activity of various anisotropic structures/shapes of AgNPs. Riss and coworkers used conventional disk assay and surface-enhanced Raman spectroscopy (SERS) to demonstrate a comparison study of the antibacterial activity between spherical, triangular, and hexagonal like-shaped of AgNPs against *E. coli* (Riss et al. 2016). Such study showed that the hexagonal shape exhibited the highest antibacterial activity, but surprisingly, the triangular AgNPs showed no activity by using either disk assay or SERS techniques (Riss et al. 2016). Other studies disclosed that the truncated triangular AgNPs or similar geometries, such as hexagons and octagons shapes displayed the highest antimicrobial efficiency (Alshareef and Laird, 2017; Chen and Carroll 2002). Pal et al. reported that the truncated triangular AgNPs

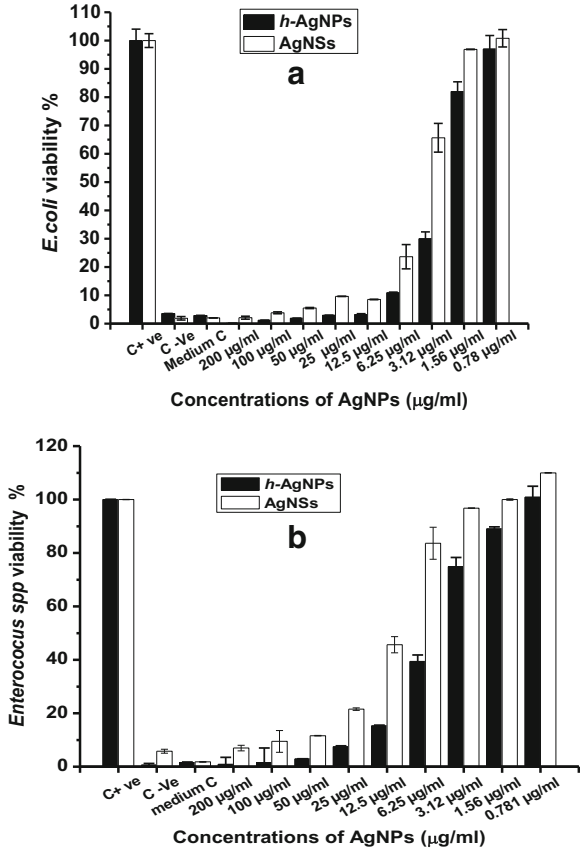

Fig. 10 The bacterial viability of two drug-resistant waterborne bacteria after 24 h treatment with AgNPs. **a** *E.coli (gram-negative)*. **b** *Enterococcus (gram-positive).* The two tested bacteria exposed to different concentrations of AgNSs or *h*-AgNPs (ranged from 200 to 0.78 μg/ml)

display *E.coli* inhibition at 1 μg/ml; however, spherical nanoparticles (NS) inhibit *E.coli* at 12.2 μg/ml, but the rod-like shape (NRs) only inhibits the *E.coli* at 50 to 100 μg/ml (Pal et al. 2007). Also, Pal et al. proved the superior efficacy of the truncated-triangular AgNPs against *E. coli* with growth inhibition at 1 μg/ml; however, spherical AgNPs (AgNSs) inhibit *E. coli* at 12.2 μg/ml, but the Ag nanorod (AgNRs) only inhibit the *E. coli* at 50 to 100 μg/ml (Pal et al. 2007).

Moreover, to the shape-dependent effect of AgNPs, we noticed a variation in the effectiveness of AgNPs in relation to bacterial species where the *Gram-negative E.coli* found more susceptible to death by AgNPs than the *Gram-positive Enterococcus*. The differences of the AgNPs efficacy are most likely due to the difference of cell wall structures; a Gram-negative cell wall is composed mainly of lipopolysaccharides and lipoproteins, whereas that of Gram-positive is typically thicker and consists of a unique type of peptidoglycans molecules (Roy et al. 2019; Silhavy et al. 2010). Therefore, *Gram-positive* bacteria are more resistant to silver nanoparticles than *Gram-negative* bacteria, since the structural nature of their cell wall is thicker and more complex than *Gram-negative* bacteria. In such a case, the cell wall of the *Gram-positive* bacterium can act as a natural barrier that prevents the penetration of both silver particles and ions (AgNPs and Ag +), which is attributed to a thick layer of the peptidoglycan layer consisting of glycan strands interconnected via peptides and anionic glycol polymers called teichoic acid. In contrast, the cell wall of *Gram-negative* bacterium is thinner with a lower content of peptidoglycan (Silhavy et al. 2010; Todar 2013).

Conclusion

Currently, the continuous spreading and thrive of MDR-bacteria in aquatic environments represent a public health threat to all life forms. This work confirmed the potent effect of two different shapes of silver nanoparticle (spherical and hexagon) against two MDR-waterborne bacteria, including *E. coli* and *Enterococcus*. Moreover, we have developed a straight forward method using the XTT test to assess the antibacterial property of nanoparticles without the need for the laborious plate count method.

Acknowledgments The authors would like to express their deepest gratitude to the National Research Centre (NRC) and Egyptian Nanotechnology Center (EGNC), Cairo University, for the technical support for this study, especially for carrying out Raman, FT-IR, and DLS/Zeta-potential measurements.

Compliance with ethical standards

Conflict of interest The authors declare that they have no conflict of interest.

References

Ali HRK, Selim SA (2016) In vitro study for comparing the cytotoxicity of silver and gold nanospheres on raw 264.7 murine macrophage cell line. J Bacteriol Parasitol 7:264

Ali HR, Ali MR, Wu Y, Selim SA, Abdelaal HF, Nasr EA, El-Sayed MA (2016) Gold nanorods as drug delivery vehicles for rifampicin greatly improve the efficacy of combating mycobacterium tuberculosis with good biocompatibility with the host cells. Bioconjug Chem 27(10):2486–2492

Alshareef A, Laird K, Cross R (2017) Shape-dependent antibacterial activity of silver nanoparticles on Escherichia coli and Enterococcus faecium bacterium. Appl Surf Sci 424:310–315

Armstrong JL, Calomiris J, Seidler RJ (1982) Selection of antibiotic-resistant standard plate count bacteria during water treatment. Appl Environ Microbiol 44:308–316

Armstrong JL, Shigeno DS, Calomiris J, Seidler RJ (1981) Antibiotic-resistant bacteria in drinking water. Appl Environ Microbiol 42:277–283

Barillo DJ, Marx DE (2014) Silver in medicine: a brief history BC 335 to present. Burns, 40:S3-S8

Bauer A, Kirby W, Sherris JC, Turck M (1966) Antibiotic susceptibility testing by a standardized single disk method. American journal of clinical pathology 45:493–496

Bibo, F. J., Birke, H., Böhm, H., Czysz, W., Gorbauch, H., Hoffmann, H. J., ... & Schneider, W. (2012). Water analysis: a practical guide to physico-chemical, chemical and microbiological water examination and quality assurance. Springer Science & Business Media

Boehm AB, Sassoubre LM (2014) Enterococci as indicators of environmental fecal contamination. In: enterococci: from commensals to leading causes of drug resistant infection. Massachusetts eye and ear infirmary,

Bush K et al. (2011) Tackling antibiotic resistance. Nat Rev Microbiol 9:894

Chen S, Carroll DL (2002) Synthesis and characterization of truncated triangular silver nanoplates. Nano lett 2:1003–1007

Clinical, and Laboratory Standards Institute (2009) Performance standards for antimicrobial susceptibility testing of anaerobic Bacteria: informational supplement. Clinical and Laboratory Standards Institute (CLSI),

Cooke MD (1976) Antibiotic resistance in coliform and faecal coliform bacteria from natural waters and effluents. N Z J Mar Freshw Res 10:391–397

Das SK, Das AR, Guha AK (2010) Microbial synthesis of multishaped gold nanostructures Small 6:1012–1021

Franci G, Falanga A, Galdiero S, Palomba L, Rai M, Morelli G, Galdiero M (2015) Silver nanoparticles as potential antibacterial agents. Molecules 20:8856–8874

Hamouda IM (2012) Current perspectives of nanoparticles in medical and dental biomaterials. journal of biomedical research 26:143–151. https://doi.org/10.7555/JBR.26.20120027

Harada T (2007) Fujiwara H Formation of rod shape secondary aggregation of copper nanoparticles in aqueous solution of sodium borohydride with stabilizing polymer. J Phys Conf Ser 1. IOP Publishing:394

Hoadley AW, Dutka BJ (1977) Bacterial indicators/health hazards associated with water: a symposium, vol 635. ASTM International, Chicago, pp 28–29

Kim JS, Kuk E, Yu KN, Kim JH, Park SJ, Lee HJ et al (2007) Antimicrobial effects of silver nanoparticles. Nanomedicine 3(1):95–101

Köhler W (1975) In: Lennette EH, Spaulding EH, Truant JP (eds) Manual of clinical microbiology. 970 S., 241 Abb., 189 Tab., 1 Tafel, vol 15. American Society for Microbiology. $15.00 Zeitschrift für allgemeine Mikrobiologie, Washington, pp 303–303

Magiorakos AP, Srinivasan A, Carey RB, Carmeli Y, Falagas ME, Giske CG et al (2012) Multidrug-resistant, extensively drug-resistant and pandrug-resistant bacteria: an international expert proposal for interim standard definitions for acquired resistance. Clin Microbiol Infect 18(3):268–281

Marathe NP, Regina VR, Walujkar SA, Charan SS, Moore ER, Larsson DJ, Shouche YS (2013) A treatment plant receiving waste water from multiple bulk drug manufacturers is a reservoir for highly multi-drug resistant integron-bearing bacteria. PLoS One 8:e77310

Mulamattathil SG, Bezuidenhout C, Mbewe M, Ateba CN (2014) Isolation of environmental bacteria from surface and drinking water in Mafikeng, South Africa, and characterization using their antibiotic resistance profiles Journal of pathogens

Mulfinger L, Solomon SD, Bahadory M, Jeyarajasingam AV, Rutkowsky SA, Boritz C (2007) Synthesis and study of silver nanoparticles Journal of chemical education 84:322

Murray G, Tobin RS, Junkins B, Kushner D (1984) Effect of chlorination on antibiotic resistance profiles of sewage-related bacteria. Appl Environ Microbiol 48:73–77

Pal S, Tak YK, Song JM (2007) Does the antibacterial activity of silver nanoparticles depend on the shape of the nanoparticle? A study of the gram-negative bacterium. Appl Environ Microbiol 73:1712–1720

Patel JB, Tenover FC, Turnidge JD, Jorgensen JH (2011) Susceptibility test methods: dilution and disk diffusion methods. In: manual of clinical microbiology, 10th. American Society of Microbiology. https://doi.org/10.1128/9781555816728.ch68

Port JA, Cullen AC, Wallace JC, Smith MN, Faustman EM (2013) Metagenomic frameworks for monitoring antibiotic resistance in aquatic environments Environmental health perspectives 122:222–228

Praveen PK, Ganguly S, Wakchaure R, Para PA, Mahajan T, Qadri K et al (2016) Water-borne diseases and its effect on domestic animals and human health: a review. International Journal of Emerging Technology and Advanced Engineering 6(1):242–245

Rai M, Yadav A, Gade A (2009) Silver nanoparticles as a new generation of antimicrobials Biotechnology advances 27:76–83

Riss TL, Moravec RA, Niles AL, Duellman S, Benink HA, Worzella TJ, Minor L (2016) Cell viability assays

Roy A, Bulut O, Some S, Mandal AK, Yilmaz MD (2019) Green synthesis of silver nanoparticles: biomolecule-nanoparticle organizations targeting antimicrobial activity. RSC advances 9:2673–2702

Shrivastava R, Upreti R, Jain S, Prasad K, Seth P, Chaturvedi U (2004) Suboptimal chlorine treatment of drinking water leads to selection of multidrug-resistant Pseudomonas aeruginosa. Ecotoxicology and environmental safety 58:277–283

Silhavy TJ, Kahne D, Walker S (2010) The bacterial cell envelope Cold Spring Harbor perspectives in biology 2:a000414

Singh S, Bharti A, Meena VK (2015) Green synthesis of multi-shaped silver nanoparticles: optical, morphological and

antibacterial properties. J Mater Sci: Mater Electron 26: 3638–3648

Sondi I, Salopek-Sondi B (2004) Silver nanoparticles as antimicrobial agent: a case study on E. coli as a model for gram-negative bacteria. J Colloid Interface Sci 275:177–182

Stiles ME, Ng LK (1981) Biochemical characteristics and identification of Enterobacteriaceae isolated from meats. Appl Environ Microbiol 41:639–645

Todar, K. (2013). Structure and function of bacterial cells

Van ME, Counotte G, Noordhuizen J (2013) Drinking water for dairy cattle: always a benefit or a microbiological risk? Tijdschr Diergeneeskd 138(86–97):99

Wakchaure R, Ganguly S, Praveen PK (2015) Role of water in livestock The Recent Advances in Academic Science Journal 1:56–60